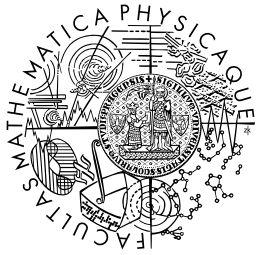

FACULTY
OF MATHEMATICS
AND PHYSICS
Charles University

BACHELOR THESIS

David Voráč

Symmetries of transition times in complex biophysical systems

Department of Macromolecular Physics

Supervisor of the bachelor thesis: RNDr. Artem Ryabov, Ph.D.
Study programme: Physics (B1701)
Study branch: General Physics (1701R026)

Prague 2020

I declare that I carried out this bachelor thesis independently, and only with the cited sources, literature and other professional sources. It has not been used to obtain another or the same degree.

I understand that my work relates to the rights and obligations under the Act No. 121/2000 Sb., the Copyright Act, as amended, in particular the fact that the Charles University has the right to conclude a license agreement on the use of this work as a school work pursuant to Section 60 subsection 1 of the Copyright Act.

In ..... date ....

Author's signature

Acknowledgement

Firstly, I'm gratefull to my coworkers from the group of Statistical Physics of Prof. Philipp Maass (University of Osnabrück) for their hospitality and all inspiring discussions during my visit. In particular, Marco who spent a good deal of his time debugging my code for my numerous simulations and pointed out everything I had done wrong until that point. Also, their tea was very tasty and the food at the university canteen was scrumptious and to kill for.

Secondly, I would like to acknowledge the help of my supervisor, RNDr. Artem Ryabov, Ph.D., to whom I'm sincerely thankful. His vital experience, insight (and also effort) helped to steer this thesis in a proper direction. Some of the computational resources were supplied by the project "e-Infrastruktura CZ" (e-INFRA LM2018140) provided within the program Projects of Large Research, Development and Innovations Infrastructures. Financial support by the Czech Science Foundation (Project No. 20-24748J) is gratefully acknowledged.

Last but not least, I'm obliged to stress the importance of the internet and its many creators of content concerning physics and mathematics. Because surely without them, the classes in elementary and high school would have been severely lacking and uninspiring and might not have incentivized me to study the quirkiness of physics.

Title: Symmetries of transition times in complex biophysical systems

Author: David Voráč

Department: Department of Macromolecular Physics

Supervisor: RNDr. Artem Ryabov, Ph.D., Department of Macromolecular Physics

Abstract: Conformational changes of biomolecules can be described as Markov processes on networks of discrete states representing minima of free energy landscapes. Network states for several types of membrane proteins and molecular motors are linked into cycles, and their reaction coordinates (represented by a "particle") jump between the cycle states predominantly in one direction with rare backward jumps occurring due to thermal fluctuations. Assuming that interactions of the particle with other degrees of freedom (other particles) cannot be neglected, we study times that it takes to complete one cycle. In particular, we compare mean times of cycle completion in and against the bias direction and show that they satisfy the universal inequality: Cycle-completion times in bias direction are never shorter than the ones against the bias. We discuss how the times depend on the interaction strength, cycle topology, quenched disorder, number of interacting particles, and check validity of our findings for two-dimensional models with canonical and grand-canonical particle reservoirs.

Keywords: Cyclic reaction networks, Markov chains, cycle-completion time, many-particle system

Contents

Introduction

Thermodynamics form a principal basis for physical and bio-chemistry where systems are inherently stochastic. Over a sufficiently long time, non-living, non-biological systems enter a state of thermochemical equilibrium. In contrast, many biological systems inside a cell function in a state of constant supply of energy and material going in and out, never achieving an equilibrium. Such state is known as a non-equilibrium steady state (NESS) [1] and is usually governed by chemical kinetics. Wide array of processes of such systems are listed in [2]: random walks and, more generally, diffusive processes, birth–death processes, growth processes on a lattice, conformational changes between discrete states of a biomolecule, molecular motors or chemical reaction networks.

The most important and widely studied example of a chemical reaction network is the central energy metabolism of the cell. It is crucial to preserving cellular functions and relies heavily on the adenosine triphosphate (ATP) for energy transfer and supply. This organic compound is found in all forms of life, abundantly and transiently so [3]. Works [4–7] give us following numbers for mitochondrial ATP synthases. There are roughly 100 processes per mitochondria, each making around 10 ATP per second and there are 10 mitochondria per cell. That gives us about 10,000 processes just making ATP. Authors estimate that the human body uses roughly 2×10^{26} transient molecules of ATP or more than the body's weight; 160 kg of ATP in a day.

If you include other self-replicating processes, the number of processes per second becomes exceedingly high, up to hundreds of thousands of times every second. Take for instance transcription of genetic information from DNA to RNA to amino acids. Each of these processes has hundreds of proteins all whirling around at quite a speed. RNA to amino acids happens at a rate of around one second per base pair, while a highly expressed gene will have thousands of copies of mRNA at any one time [8].

The mentioned cellular processes are self-renewing and typically realized with a help of biomolecules. These include enzymes, molecular motors and other organic macromolecules. Yet, they are not always working impeccably in the intended direction of the function they serve. Instead, they are inherently error-prone and susceptible to thermodynamic fluctuations, which impacts their efficiency. Although the kinetics of cyclic reactions have been studied extensively in the past, not as much in the context of mutual interaction between biomolecules.

Motivated by cyclic chemical reactions occurring in the aforementioned processes, we study a Markov processes on networks of discrete mesoscopic states representing minima of free energy landscapes [9–11]. For instance, a motor protein, myosin V [12], moves intracellular vesicles around cells along an actin filament powered by the hydrolysis of ATP. Myosin's movement consists of series of attachments and detachments of its two myosin heads, akin to a human walking. The myosin walk can be broken down into three mesostates and thus be represented as a three-state unicyclic Markov network. However, this process is reversible [13–15] which together with its stochastic nature implies that a backstep is always a real, albeit low-chance, possibility.

Requirement for any process to be microscopically reversible is conveniently

incorporated into our Markov network model via a condition known as *local detailed balance* [2, 16]. A surprising consequence of satisfying this condition is an equality of cycle-completion times (*i.e.* backward and forward cycles are completed, on average, with identical times). It has been rediscovered and exploited by several authors [17, 18] notably in the context of membrane transport [19], chemical kinetics of enzymes [20] and molecular motors [21, 22]. Our main goal is to test, under which conditions this equality could be violated.

We devise a simple model of a Markov process on network states linked into cycle and with reaction coordinates represented as a particle. We thoroughly investigate the effect of interactions of a particle with other degrees of freedom, *i.e.*, other particles. Particularly strong emphasis is put on studying a mean values and variances of times of cycle completion, which may aid in a better understanding of efficiencies of biochemical cycles far from equilibrium.

The structure of this thesis is as follows. In Chapter 1, we recapitulate the basic principles of Markov chains and demonstrate their application in modeling the aforementioned biological systems. We also present the basics of kinetic Monte Carlo method. In the latter part of the chapter, the equality of cycle-completion times in a cycle is shown and verified using the kinetic Monte Carlo method. In Chapter 2, we discuss the impact of introducing additional interacting particles to a unicyclic network. We demonstrate and explain a remarkable inequality of corresponding cycle-completion times. In Chapter 3, we examine if the inequality of cycle-completion times can be generalized to two dimensions. We investigate this for canonical and for grand-canonical reservoir coupled to the reaction network.

1. Kinetics of biochemical cycles

The evolution of biochemical reaction networks, particularly those of enzymes or molecular motors which function in NESS, depend on specific couplings to reservoirs (*e.g.* chemical concentration, load) and on dynamics inherent to the particular system (*e.g.* type of enzyme, molecular motor). Each model of such nonequilibrium processes has to incorporate a description of these couplings and of the dynamics. It is often theoretically simpler to represent the effect of the reservoirs in stochastic terms and reduce the complex dynamics to a Markov jump process [16, 23, 24].

Markov jump process represents a reaction network as a random walker occupying different discrete states (colllectively called statespace [25]) over the course of time which is treated as a continous property. The changes between individual states are called transitions and have *rates* associated with them [26]. These are denoted by w_{ij} and represent a rate at which the system transitions from state i to state j in an infinitesimal time interval $\mathrm{d}t$. Note that transitions $i \to j$ and $j \to i$ are distinct from each other and generally have a separate transition rate assigned to each.

For the transition rates to be compatible with real-world physics of biochemical reactions, one must subject them to a concept of thermodynamics. In the case of an equilibrium, a commonly known principle of microscopic reversibility, or detailed balance, must hold [27]. The principle states that when a system is at an equilibrium (a state of zero entropy production), the frequency of transitions is the same in both directions for each individual reaction step. For Markov chains specifically, this can expressed as

$$\pi_i w_{ij} = \pi_j w_{ji} \tag{1.1}$$

where π_i and π_j are the equilibrium probabilities of being in states i and j, respectively [28]. This relation amounts to a time-reversal symmetry of a stationary process.

Alternatively, if there is not genuine equilibrium, one expects the detailed balance to be broken. However, for a nonequilibrium system it is instead replaced by the condition of *local detailed balance* [2, 11, 16], which can be expressed as [29]

$$\frac{w_{ij}}{w_{ji}} = \mathrm{e}^{-\beta \Delta E(i \to j)}, \tag{1.2}$$

where $\Delta E(i \to j)$ is an energy function. The function $\Delta E(i \to j)$ includes an energy difference between states (sites) i and j, and the work done by external non-conservative driving forces which are frequently of a chemical origin [30] or, represent an external load.

The aggregate of these driving forces acting on the system (*e.g.* the chemical reaction, diffusion process,...) is called a drift. The drift biases the random walker to move in a certain direction. Even though, at a given instant in time, the system may step in any direction, over many steps the system will, on average, move in the direction of the drift.

In a living cell, the drift takes the form of a constant and continous supply of material and energy. Such environment allows the reaction to renew and occur cyclically.

1.1 Gambler's ruin problem

Markov processes with a discrete statespace can be easily visualised with the help of graph theory. Vertices of a graph represent states of the system while directed edges between the vertices represent possible transitions.

As an illustration, consider a particle which can move on a one-dimensional lattice between $2n+1$ sites numbered from $-n$ to n (see Fig. 1.1). The particle can jump only between nearest neighboring sites. It starts its random walk from $x(t=0)=0$, and stops once it reaches an absorbing boundary at n or $-n$ for the first time. Furthermore, a drift f is present which biases the particle to move to the right if $f>0$. This problem might be familiar to the reader, as it is simply an example of a biased discrete random walk with absorbing boundaries, or more concisely, the *Gambler's ruin problem* [31, 32].

The most natural question to ask in this scenario is: What is the probability for a particle to reach the absorbing boundary at n? The question that usually follows is: What is the mean time it takes a particle to reach the absorbing boundary? In mathematics this is commonly known as the conditional first-passage time [33]. By the condition we mean that reaching of the preferred absorbing boundary is guaranteed. If that is the case, then the trajectory of a particle is called successful.

In the context of physical chemistry and cyclic biochemical reactions, the conditional first-passage time of Gambler's ruin problem directly corresponds to a transition time of a reaction, *i.e.*, the time it takes a system to complete a cycle. In this framework, it is more appropriate and to avoid any confusion with time intervals between individual transitions, to refer to the conditional first-passage (or transition) time as a *cycle-completion time*, denoted in this thesis by τ. Additionaly, if an absorbing boundary in the bias direction is reached, we denote it by τ_0^+. Conversely, if an absorbing boundary against the bias direction is reached, we denote it by τ_0^-.

To show a direct analogue between the Gambler's ruin problem and a cyclic reaction network, compare Fig. 1.1 and 1.2. The linear chain with $2n-1$ sites is de facto a representation of two identical processes of length n linked together. By identifying an initial site $x(t=0)=0$ with both absorbing boundaries and other sites accordingly, the Gambler's ruin problem can be reconstructed as a cyclic Markov chain shown in Fig. 1.2. A particle is absorbed once it completes a cycle (*i.e.* the particle jumps through all sites back to its initial site making a "full revolution") either in or against the drift bias. For brevity's sake, we shall refer to cyclic model statespace as 4-cycle, 5-cycle and so on depending on the number of sites.

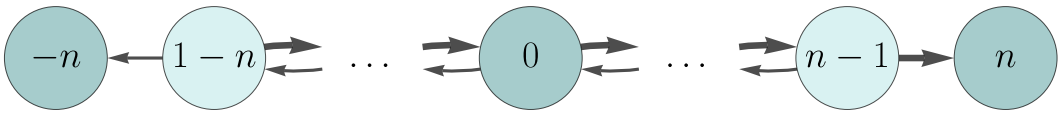

Figure 1.1: A graph of a Markov process with $2n+1$ sites linearly linked together with two absorbing boundaries on either end. Emboldened graph edges represent transitions favored by the positive value of drift f.

1.2 Kinetic Monte Carlo

In the case of Gambler's ruin problem, and therefore also in a 4-cycle, it is possible to determine the mean conditional first-passage time $\tau_0^{\pm}$ analytically [26, 34]. The same approach can be used to solve problems on a two-dimensional lattice, although the exact form of the solution quickly becomes unwieldy to express explicitly. For systems with multiple particles, finding the exact solution is simply not possible. In this thesis, we will resort to finding cycle-completion times using a simulation.

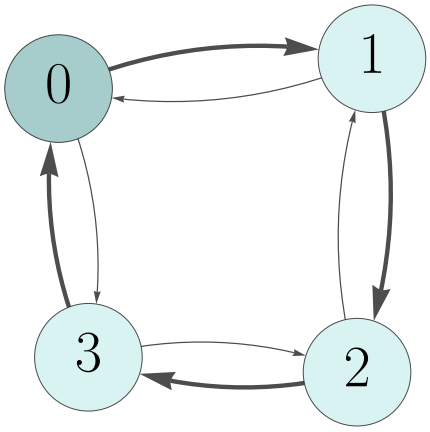

Figure 1.2: The 4-cycle: A unicyclic graph of four sites. Emboldened graph edges represent transitions favored by the positive value of drift f.

The most straightforward method, and the one we shall use, is the well-known *kinetic Monte Carlo* (KMC). KMC is a computer simulation intended to simulate the time evolution of some stoachastic process. It is widely used both for equilibrium and non-equilibrium processes [30, 35] and is based on the same principles as dynamic Monte Carlo and Gilespie's algorithm [36, 37].

In order to design a proper KMC simulation, individual transition rates are typically needed to be known and inputed into the simulation beforehand. The KMC by itself cannot predict them and in practical application these have to be acquired from other methods, such as diffusion experiments, molecular dynamics simulations or optical studies [38].

For all of our models, we define universally transition rates of a single particle from a site i to j as follows:

$$w_{ij} = \begin{cases} a_{ij}\mathrm{e}^{\frac{\beta}{2}f+\frac{\beta}{2}(\varepsilon_i-\varepsilon_j)} & \text{for transitions in the direction of positive } f, \\ a_{ij}\mathrm{e}^{-\frac{\beta}{2}f+\frac{\beta}{2}(\varepsilon_i-\varepsilon_j)} & \text{otherwise,} \end{cases} \tag{1.3}$$

where $a_{ij} = a_{ji}$ are constants representing the frequencies of unbiased transitions, β is the inverse thermal energy ($1/\beta = \mathrm{k_B}T$ where $\mathrm{k_B}$ is the Boltzmann constant and T is temperature), f denotes the drift, and the term $(\varepsilon_i - \varepsilon_j)$ represents an energy difference between sites i and j.

In all simulations, we set $\beta = 1$, which means ε_i and f will be given in units of $\mathrm{k_B}T$. Parameters a_{ij} and ε_i will be used in Sec. 2.6 to model local inhomogenities of dynamics. Otherwise, we shall set $a_{ij} = 1$, $\varepsilon_i = 0$, and call this scenario a *homogeneous n-cycle*.

Defining transition rates in this manner guarantees that the local detailed balance (1.2) is satisfied. Thus, our model can be interpreted as time-reversible and compatible with thermodynamic principles.

The KMC algorithm that we use consists of ten steps:

1. Set the time to $t = 0$.

2. Set the initial state $x(t = 0) = x_0$ and the absorbing boundaries.

3. Form a list of transition rates w_{xj} from the current state x to all possible states $j = 1, \ldots, N_x$.

4. Calculate a cumulative sum $Z_{xj} = \sum_i^j w_{xi}$. The total rate of transition from the state x is $Z_x = Z_{xN_x}$.

5. Generate a uniform random number $r_1 \in (0, 1]$.

6. Find out which transition $x \to j$ happens by finding j for which:

$$Z_{x,j-1} < r_1 Z_x \leq Z_{xj}.$$

7. Generate a new uniform random number $r_2 \in (0, 1]$.

8. Update the time with $t = t + \Delta t$, where $\Delta t = \frac{1}{Z_x} \log(\frac{1}{r_2})$ is a dwell time.

9. Carry out the transition $x \to j$.

10. If $x(t) = \pm n$, record time as the cycle-completion time: $\tau = t$, and set time to $t = 0$. Otherwise return to step 3.

The step 6 is justified since the rates directly correspond to the probability p_{xi} of transition $x \to i$ such that

$$p_{xi} = \frac{w_{xi}}{Z_x}. \tag{1.4}$$

We discard any trajectory ending in a non-preferred absorbing boundary. This process is repeated until a desired number of successful trajectories is obtained.

Now that we have established all the necessary preliminaries, it is possible to translate any Markov process into a KMC simulation. All coding was done in MATLAB R2019B and full written code can be found in the A Appendix at the end of this thesis.

1.3 Equality of cycle-completion times

The principle of time reversal operates on the level of single trajectories. To show this, consider a trajectory of a particle in a 4-cycle: $\{x(t)\}$, where $0 \leq t \leq t'$. The reversed trajectory is defined as $\{x^\dagger(t' - t)\}$ with the transitions in the opposite direction of the original. If a trajectory was completed in the bias direction, then its reversed counterpart was completed instead against the bias direction.

Any trajectory of a single diffusing particle making a transition between two end points of an interval can be divided into two segments, which we call direct-transit and looping parts. The former is the final segment of the trajectory, when the particle goes from one end point of the interval to the opposite end point, without retouching the starting point. The rest of the trajectory is the looping part.

It has been proven, that mean first-passage time of both looping and direct-transit part of the trajectory is identical for downhill (in the bias) and uphill (against the bias) transitions [39]. Thus, we should see equality of $\tau_0^+(f)$ with $\tau_0^-(f)$. That is the particle completes a cycle against the bias just as fast as in the bias direction.

As previously stated in Sec. 1.2, times $\tau_0^{\pm}(f)$ can be derived analytically or by using KMC simulations. Figure 1.3 shows the plot of $\tau_0^{\pm}(f)$ determined by the KMC method for a 4-cycle. A clear equality is indeed evident:

$$\tau_0^{+}(f) = \tau_0^{-}(f) = \tau_0(f) \tag{1.5}$$

In the presence of the drift f, the mean cycle-completion time decreases compared to its value at $f = 0$. As $|f| \to \infty$, the mean cycle-completion time tends zero.

Moreover, we can observe that functions $\tau_0^{\pm}(f)$ are symmetrical in relation f. This is simply a consequence of their equality because changing the parity of f equates to switching absorbing boundaries. Hence

$$\tau_0^{\pm}(f) = \tau_0^{\mp}(f) = \tau_0^{\pm}(-f) \tag{1.6}$$

Generalizations can be made for cycles of different length; shorter cycles have a smaller values of $\tau_0^{\pm}(f)$ while longer ones have greater, but both display the same equality and symmetry.

The symmetry and equality of $\tau_0^{\pm}$ is one of the most surprising consequences of local detailed balance condition [40]. It has been rediscovered and exploited by several authors [17, 18], notably in the context of membrane transport [19], chemical kinetics of enzymes [20] and molecular motors [21, 22]. In more recent papers [41, 42] equality of cycle-completion times was found not to be always the preserved. In the latter paper, the authors state that the symmetry is broken specifically for many-particles systems with a short-range repulsive interaction.

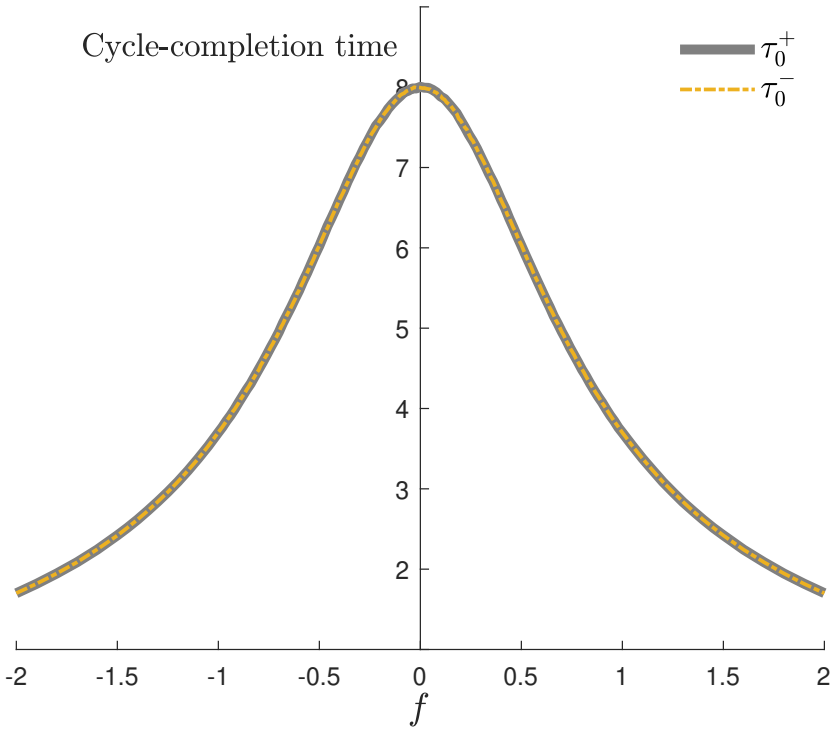

Figure 1.3: Mean cycle-completion times $\tau_0^{+}(f)$, and $\tau_0^{-}(f)$ for a 4-cycle. Parameters used: $\beta = 1$, $a_{ij} = 1$, $\varepsilon_i = 0$ number of KMC trajectories: 10^6.

2. Interacting particles on a ring

Expanding upon the previous chapter, it was shown that cycle-completion times $\tau_0^+(f)$ and $\tau_0^-(f)$ of a 4-cycle with one particle (or a cycle of any length for that matter) are both identical and symmetrical in relation to an external drift f. This was a result of the microspic reversibility. Yet, in most *in vivo* processes, it is highly expected that the particle would interact with other ones diffusing nearby. An endeavour to determine $\tau^{\pm}$ in the presence of other particles becomes a matter of great curiosity. Will the equality $\tau^+(f) = \tau^-(f)$ hold for systems with two or more interacting particles? In this chapter, we will answer this question for a one-dimensional case.

We shall consider two identical particles performing a random motion on a 4-cycle shown in Fig. 1.2. Without the interaction, each particle moves exactly as the one discussed in the previous chapter with transition rates w_{ij} given in (1.3). The particles interact either if they occupy the same site, or the nearest neighboring ones. The interaction affects transition rates of the two-particle system. The rate W_{ij} of the transition, where a particle jumps from the site i to the site j depends on the position of the other particle in the following manner:

$$W_{ij} = \begin{cases} w_{ij}\mathrm{e}^{\frac{\beta}{2}g} & \text{if particles occupy the same site,} \\ w_{ij}\mathrm{e}^{-\frac{\beta}{2}g} & \text{if the site } j \text{ is occupied by the other particle,} \\ w_{ij} & \text{if none of the above.} \end{cases} \tag{2.1}$$

The parameter g can be understood as the potential energy of interaction. The two-particle system gains energy $+g$ when the particles occupy the same site. For negative values of g, the interaction is attractive, while for positive values it is repulsive. Form of rates W_{ij} is such that the two-particle dynamics obeys the local detailed balance condition (1.2).

We shall consider exclusively non-equilibrium steady-state dynamics. As such, the issue of initial conditions must be addressed. In the case when a Markov process is space-homogeneous (translationally invariant), the probability distribution of particles' initial position can be analytically derived for any value of drift f [26]. Generally, however, it is better to employ a less exact but more simple approach taking advantage of the large number of Monte Carlo simulation runs. For the first simulation run, we generate random initial conditions and let the system evolve. When the first particle completes a cycle in either direction, a next simulation run is initiated without changing any particle's position. Hence, the system quickly reaches a steady state in just a few runs without any need for external adjustment [29].

For a more complicated case of a non-homogeneous 4-cycle, see Sec. 2.6.

2.1 Summary of main results

Using the KMC (as introduced in Sec. 1.2) to determine $\tau^+(f)$ and $\tau^-(f)$ of 4-cycle with two interacting particles has yielded results shown in Figs. 2.1 for repulsion ($g = -4$) and 2.2 for attraction ($g = +4$). Both figures are accompanied by a plot of mean cycle completion time with no interaction ($g = 0$) denoted by $\tau_0(f)$. In both instances, the results are unexpected and counterintuitive.

Here is a brief summary of the six most important observations, each of which will be discussed and expanded upon in its own section of this chapter.

i) For space-constant single-particle transition rates, every interaction between particles slows down the cycle-completion process,

$$\tau^{\pm}(f) \geq \tau_0(f). \tag{2.2}$$

ii) An inequality

$$\tau^{+}(f) \geq \tau^{-}(f) \tag{2.3}$$

holds for any value of interaction parameter, g, *i.e.* trajectories are faster against the direction of the bias than along. The equality of τ^+ and τ^- holds either without any bias:

$$\tau^{+}(f=0) = \tau^{-}(f=0), \tag{2.4}$$

or, naturally for $g = 0$, see Eq. (1.5).

iii) For strongly driven systems, we observe

$$\lim_{|f|\to\infty} \frac{\tau^{-}(f)}{\tau_0(f)} = 1, \tag{2.5}$$

that is, a particle completing a cycle against a strong bias behaves very similarly to non-interacting particle regardless of a number of other particles.

Cycle-completion times in the bias direction behave such that

$$\lim_{|f|\to\infty} \frac{\tau^{+}(f)}{\tau_0(f)} = h(g), \tag{2.6}$$

where $h(g)$ is a function of g, $h(g) > 1$.

iv) Fluctuations of cycle-completion times are most pronounced in the absence of drift ($f = 0$) and exponentially decrease with increasing $|f|$.

v) Non-homogenities of the transition rates do not break the symmetry relative to f: $\tau^{\pm}(f) = \tau^{\pm}(-f)$; the inequality $\tau^{+}(f) \geq \tau^{-}(f)$ also holds. However, in some special cases the inequality (2.2) can be violated.

vi) Inequality (2.3) becomes stronger with an increasing number of particles in the system. Although $\tau^{\pm}(f)$ may also increase as per the point i) of this summary.

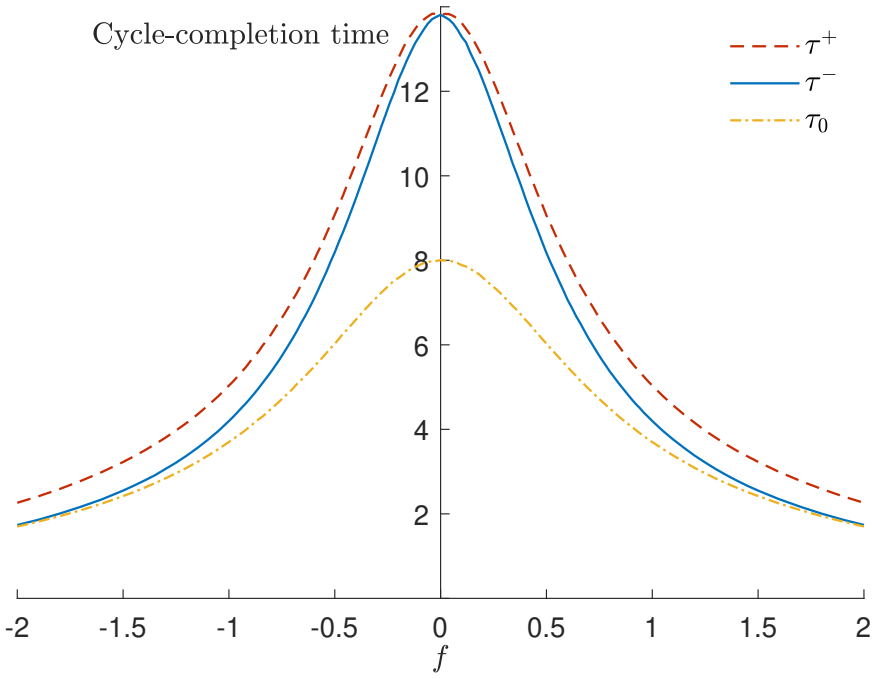

Figure 2.1: Mean cycle-completion times $\tau^+(f)$, and $\tau^-(f)$ for a 4-cycle with two particles interacting repulsively ($g = 4$), and $\tau_0(f)$ corresponding to $g = 0$. Parameters used: $\beta = 1$, $a_{ij} = 1$, $\varepsilon_i = 0$, number of KMC trajectories: 10^6.

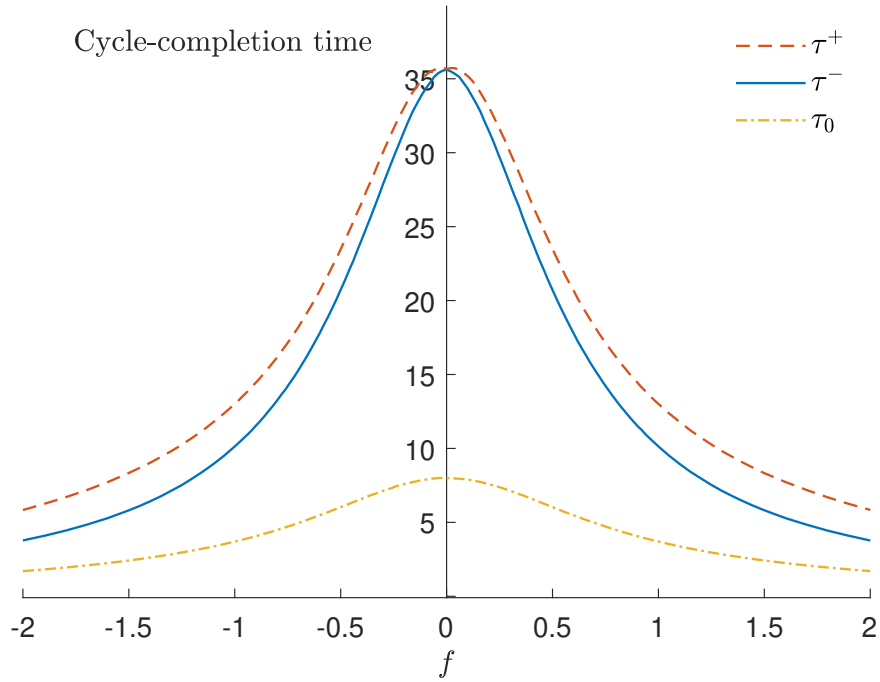

Figure 2.2: Mean cycle-completion times $\tau^+(f)$, and $\tau^-(f)$ for a 4-cycle with two particles interacting attractively ($g = -4$), and $\tau_0(f)$ corresponding to $g = 0$. Parameters used: $\beta = 1$, $a_{ij} = 1$, $\varepsilon_i = 0$, number of KMC trajectories: 10^6.

2.2 Interaction as an inhibitor

Why does interaction cause such a large difference between cycle-completion times $\tau^{\pm}$ and τ_0? The most noticeable increase is for $f = 0$, where cycle-completion times attain their maximal values. Longer cycle-completion times mean that particles have more occassions to meet and interact with each other.

In the case of attractive interaction, it is very probable for the two particles to exist in the same site. Such situation has a very low total rate Z_x and thus a longer dwell time Δt due to the step 8 of KMC algorithm. Increase in dwell time Δt in the case of same site occupancy is not compensated by a corresponding decrease in a situation where the particles are neighboring each other. Thus, the total of the two dwell times is higher.

In the case of repulsion, it is more likely for the particles to be neighboring each other and less so to be occupying the same site. Nevertheless, the same argument still holds and the total time is higher. Note that is regardless of the second particle's position. It could be either in front of the first particle ("blocking" it) or behind it ("trailing" it). The greater the interaction energy g, the more pronounced the effect is.

To give a concrete proof, we will use only Definition (2.1) and suppose a cycle with zero energy difference between sites ($\varepsilon_i = 0$ for any i) and two-particle interaction. When particles are interacting, the total rates are equal to

$$Z_x = \begin{cases} 2(w_{ij} + w_{ji})\mathrm{e}^{\frac{\beta}{2}g} & \text{if they occupy the same site,} \\ (w_{ij} + w_{ji})(1 + \mathrm{e}^{-\frac{\beta}{2}g}) & \text{if they occupy neighboring sites.} \end{cases} \tag{2.7}$$

And consequently we have

$$\frac{1}{2(w_{ij} + w_{ji})\mathrm{e}^{\frac{\beta}{2}g}} + \frac{1}{(w_{ij} + w_{ji})(1 + \mathrm{e}^{-\frac{\beta}{2}g})} \geq \frac{1}{2(w_{ij} + w_{ji})},$$

$$1 + \frac{2\cosh\left(\frac{\beta}{2}g\right)}{\mathrm{e}^{\frac{\beta}{2}g} + 1} \geq 1, \tag{2.8}$$

where both sides of the inequality represent a sum of dwell times when two particles are in the same site and in neighboring sites. The left side assumes $g \neq 0$ while the right side assumes the opposite, $g = 0$.

Thus, $\tau^{\pm}(f)$ is always greater than $\tau_0(f)$. However, this inequality can be violated for non-homogeneous cycles where we must take into a consideration different energies of sites (see Sec. 2.6).

2.3 Inequality of cycle-completion times

While $\tau_0^{\pm}(f)$ are identical, for two-particle system a noticeable inequality of $\tau^{+}(f)$ and $\tau^{-}(f)$ is observed in Figs. 2.1 and 2.2. Puzzlingly, $\tau^{-}(f)$ is always smaller than $\tau^{+}(f)$, that is the cycle is completed faster against the bias than along. Furthermore, the same inequality is observed for both repulsive and attractive interaction. This counterintuitive behavior can be understood by conducting the following thought experiment.

Consider all successful trajectories completing a 4-cycle against the bias in a single-particle system, that is those determining τ_0^{-}. Now, consider the same

trajectories but with another particle present. The second particle will, on average, move consistently in the direction of the drift f towards the first particle. If the two particles meet, they will either neighbor each other first (most probable for the repulsive interaction, $g < 0$) or commence their trajectories at the same site (most probable for the attractive interaction, $g > 0$).

If the particles meet and the interaction is repulsive, then the first particle is blocked. The second particle reduces the first one's transition rate by a factor of $e^{-\beta g/2}$. The first particle either overcomes the blocking with longer dwell time or is pushed backsliding its progress. A similar event occurs if the interaction is attractive. Instead of being blocked, it is instead pulled along by the second particle in the bias direction. The effect is the most pronounced when both values of f and g are large. In both instances first particle's chances of moving against the bias and completing the cycle succesfully are reduced. Therefore, the most surviving trajectories are those with fewer times particles meeting or it never happening at all.

Let us contrast this with the trajectories in the bias direction. Unlike before, drift forces carry both particles at roughly the same speed in the bias direction with both particles following a relatively straighforward trajectory. Sometimes particle might take a quick "detour" going against the bias, but a majority of the simulated trajectories complete cycle regardless of interaction.

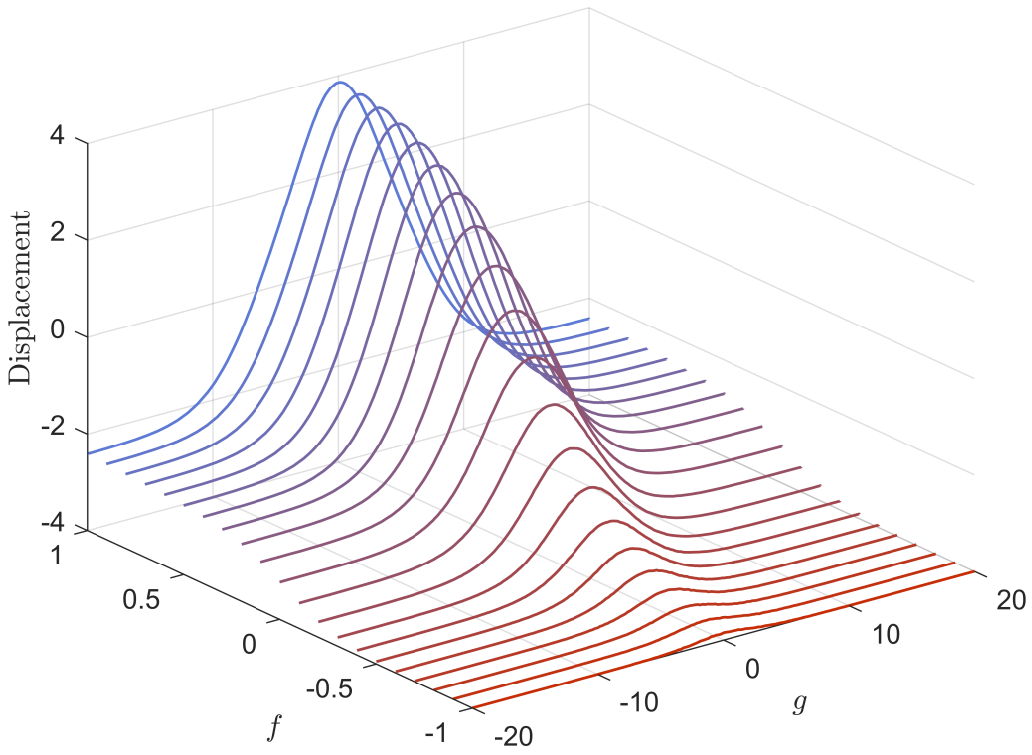

Figure 2.3: Displacement of the second particle from its initial position in a 4-cycle with trajectories against bias for positive values of f (colored blue) and in bias for negative values of f (colored red). Parameters used: $\beta = 1$, $a_{ij} = 1$, $\varepsilon_i = 0$, number of KMC trajectories: 10^6.

In conclusion, trajectories determining τ^- experience less interaction compared to trajectories determining τ^+. If we take into account that any kind of interaction

increases cycle-time, as we have shown in (see Sec. 1.2), we should see some disparity between $\tau^+(f)$ and $\tau^-(f)$.

Should our hypothesis to hold, we expect the number of interactions to be decreasing with g for trajectories determining τ^-. This can be true only if the second particle does not move freely in the direction of the drift. In Fig. 2.3 we indeed observe displacement of the second particle from its initial position decreasing for trajectories completed against the drift (blue-colored). For small values of $g \approx 0$, the particle moves freely in the direction of the drift making the maximum amount of four jumps in one direction. It is not affected in any way by the other particle. As g increases, so does the number of particles meeting. Most of these meetings prevent, or at least hamper, a succesful completion of the cycle.

First particle's trajectory requires it move against the drift a set number of jumps. Whereas second particle is bound by no such requirement. If the trajectory is to be completed against the bias, the second particle's displacement must be gradually reduced to prevent meeting with the other particle as g increases.

If we increase g even further, all the trajectories with the particles meeting will be unsucessful. Thus, to avoid meeting first particle entirely, the second particle must now also move against bias. Figure 2.3 shows this to be happening for $|g| > 5$. However, jumping against bias has a very low probability. Hence, the second particle will try to minimize the number of jumps it has to make against the bias; down to a mean of -2. Starting from a site numbered 1 in Fig. 1.2, neighboring $x_0 = 0$, it executes two jumps against the bias, namely $1 \to 0$ and $0 \to 3$. No meeting of particles occurs.

For τ^+, we should expect the displacement to be equal to the displacement of the first particle (i.e. number of sites in the cycle). Both particles are identical thus the probability of moving next is $\approx 1/2$, which is only negligibly affected by their mutual interaction. The confirmation can be found in Fig. 2.3 for $f < 0$ plots (colored red).

2.4 Strongly driven cycles

In Fig. 2.1, we observe values of $\tau^-(f, g = +4)$ approaching those of $\tau_0(f)$ for strongly driven cycles. The same can be said in the case of attractive interaction ($\tau^-(f, g = -4)$) shown in Fig. 2.2. Although the values tend to $\tau_0(f)$ more slowly than in the case of repulsion. As discussed earlier in Sec. 2.3, the only surviving trajectories determining $\tau^-(f)$ for very large $|f|$ are those without any kind of interaction occurences. Hence, any trajectories in multiple-particle strongly driven system completing a cycle against the bias are equivalent to a single-particle case.

A similar trend can be observed for $\tau^+(g = \pm 4)$. We have increased the range of f in KMC simulation to $(-10, 10)$ as shown in Fig. 2.4 with a logarithmic scale for several values of g. For roughly $f > 2$, all $\tau^+(f)$ and $\tau_0(f)$ are decreasing exponentially by a factor of $\beta/2$, but there is a noticeable difference between individual plots. Times $\tau^+(f)$ are $h(g)$ multiple of the single-particle case $\tau_0(f)$, as mentioned in Eq. (2.6).

Virtually all trajectories in strongly driven cycles comprise of exactly four jumps, namely $0 \to 1 \to 2 \to 3 \to 0$. Both particles can freely interact (in contrast to those determining $\tau^-(f)$). The total rates Z_x (see Sec. 2.2) are therefore affected,

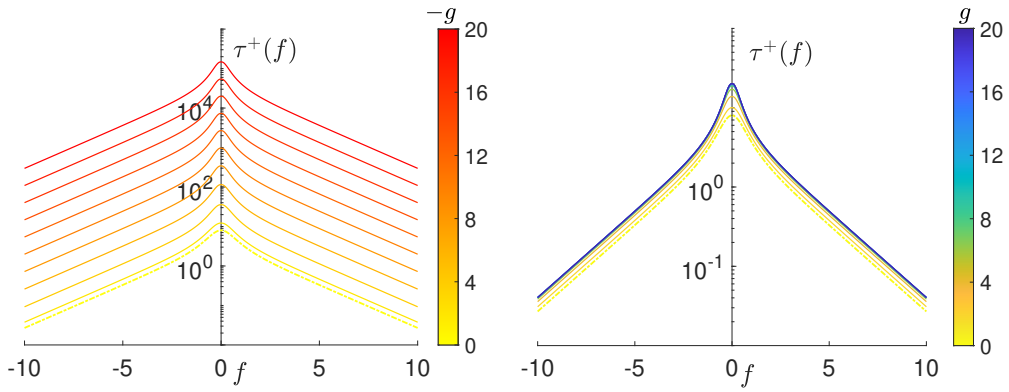

(a) Attraction. (b) Repulsion

Figure 2.4: Plots of $\tau^+(f)$ for a system with two particles interacting with various values of g. A difference between them and $\tau_0(f)$ is displayed. Parameters used: $\beta = 1$, $a_{ij} = 1$, $\varepsilon_i = 0$, number of KMC trajectories: 10^6.

which results in the difference dependent on the value of g. For attraction, it is substantial and unbounded while for repulsion, it is very small and bounded.

If we take a look at the inequality (2.8), the reason becomes apparent. Whenever the two particles interact, their dwell times are multiplied by the left side of the inequality (2.8). For $g < 0$, it is unbounded, while for $g > 0$ it is bounded and tends to 2. The left side of inequality (2.8) does not equate to the function $h(g)$ in Eq. (2.6), however. Because we do not know the mean number of interaction occurences per trajectory.

But what is the reason for $\tau^+(f)$ to be decreasing exponentially by a factor of $\beta/2$? Take into account that all trajectories comprise of four jumps and also $W_{i,i+1} \gg W_{i,i-1}$ and thus the right side of inequality is negligible. Then the dwell time $\Delta t \propto \mathrm{e}^{-\beta f/2}$ and by the same logic $\tau^+ \propto 4\mathrm{e}^{-\beta f/2}$ which is exactly what we wanted to show.

2.5 Fluctuations of trajectories

Let us analyze how much do individual trajectories differ from each other in terms of length and the order of transitions. Figure 2.5 shows a standard deviation of $\tau^-(f)$ and $\tau^+(f)$ both peaking at $f = 0$ and also manifesting the previously encountered inequality. As f increases, fluctation rates plummet indicating only a few typical trajectories are dominating. Some of them are visualised for $f = 2$ in Fig. 2.6 which shows a small sample of four. The trajectories indeed do not differ from each other significantly, especially in terms of transition order of the first particle. Conclusive confirmation of few trajectories dominating can be found in Table 2.1 and 2.2.

Comparing the trajectories in a Table 2.2 with trajectories in Table 2.1, suggests the two particles are interacting more often for $\tau^+(f)$ than $\tau^-(f)$. One can prominently see such tendency in the trajectories of the second particle: when a cycle is completed against the bias, the second particle always starts at the site 1 and almost never transitions to the site 0. Otherwise, it would mean blocking the first particle, unlike in the case of τ^+ where the site 0 is almost always occupied

at some point in time. These results are in order with our hypothesis in Sec. 2.3.

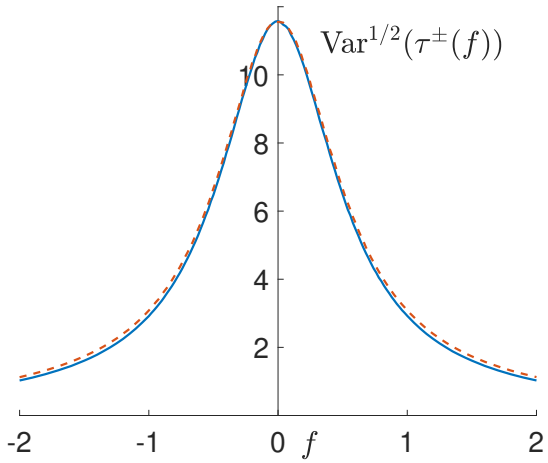

Figure 2.5: Standard deviation of $\tau^{\pm}(f)$ with repulsive interaction ($g = +4$) also displaying inequality (2.3). Parameters used: $\beta = 1$, $a_{ij} = 1$, $\varepsilon_i = 0$, number of KMC trajectories: 10^6.

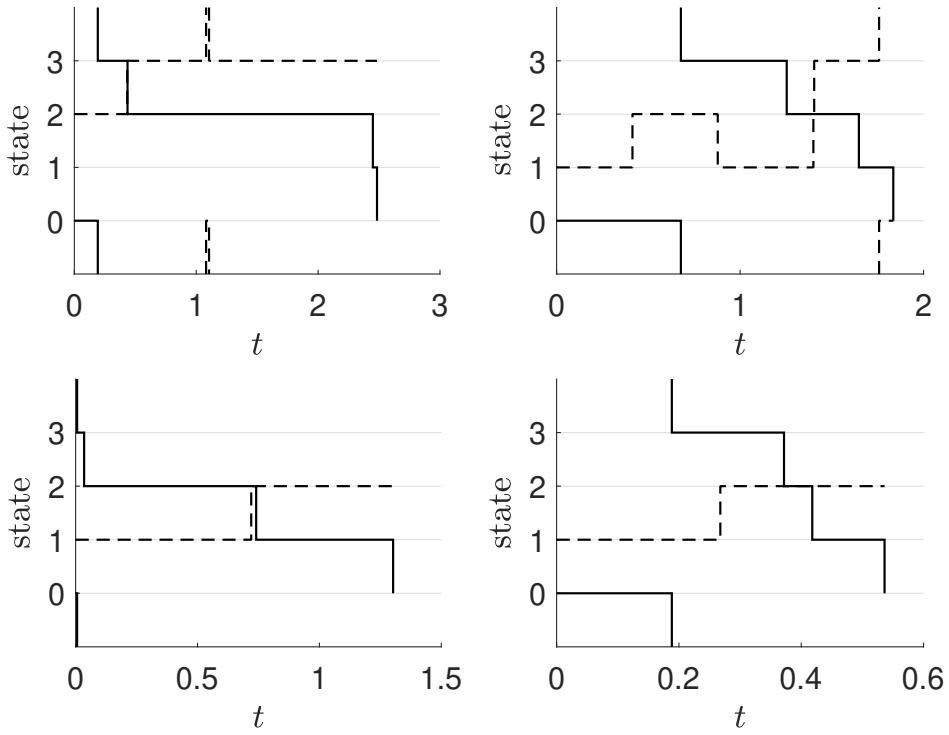

Figure 2.6: Sample trajectories of the second particle (dashed line) and the first particle (full line) completing a cycle against bias ($|f| = 2$) with the two particles interacting repulsively ($g = +4$). Parameters used: $\beta = 1$, $a_{ij} = 1$, $\varepsilon_i = 0$.

Table 2.1: Approximate prevalence of constituent particles' trajectories in two-particle system. Cycle is completed against the bias direction and the two particles are interacting repulsively ($g = +4$). Number of KMC trajectories: 10^4.

1st particle's trajectory	**Prevalence**
0, 3, 2, 1, 0	70 %
0, 3, 0, 3, 2, 1, 0	6 %
0, 3, 2, 3, 2, 1, 0	5 %
0, 3, 2, 1, 2, 1,0	5 %
2nd particle's trajectory	**Prevalence**
1, 2, 3	11 %
1, 2, 3	10 %
2, 3	5 %
1	4 %

Table 2.2: Approximate prevalence of constituent particles' trajectories in two-particle system. Cycle is completed in the bias direction and the two particles are interacting repulsively ($g = +4$). Number of KMC trajectories: 10^4

1st particle's trajectory	**Prevalence**
0, 1, 2, 3, 0	58 %
0, 1, 2, 3, 2, 3, 0	7 %
0, 1, 0, 1, 2, 3, 0	7 %
0, 3, 0, 1, 2, 3, 0	7 %
0, 1, 2, 1, 2, 3, 0	7 %
2nd particle's trajectory	**Prevalence**
1, 2, 3, 0, 1	10 %
2, 3, 0, 1	10 %
1, 2, 3, 0, 1, 2	9 %
2, 3, 0, 1, 2	8 %
1, 2	2 %

2.6 Non-homogeneous cycles

Recalling the Definition (1.3) of transition rates w_{ij}, we have two ways how to introduce non-homogenity (quenched disorder) into a system: that is via changing a_{ij} and ε_i. In this section, we will examine both of them.

Slowed/accelerated transition

First is the possibility of different frequencies of transition between sites i and j with $\varepsilon_i = \varepsilon_j$. In the context of biochemical reactions, parameters a_{ij} quantify heights of (free) energy barriers between sites i and j. Transition $i \leftrightarrow j$ can be either slowed down ($a < 1$) or accelerated ($a > 1$) compared to $a = 1$. However, equality $a_{ij} = a_{ji}$ must hold since we assume the local detailed balance condition to be satisfied.

Figure 2.7 shows result for one slowed (a) and one accelerated (b) transition

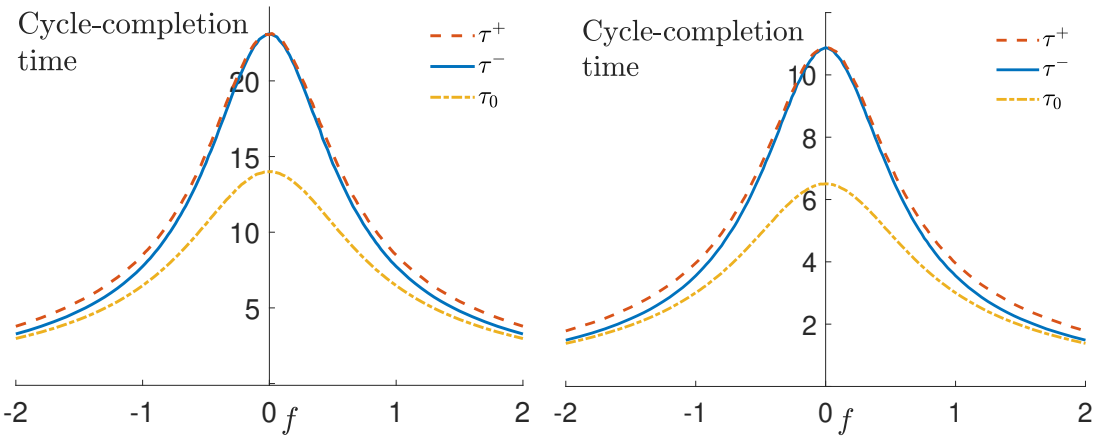

(a) Slowed transition ($a = 0.25$)

(b) Accelerated transition ($a = 4$)

Figure 2.7: Comparison of cycle-completion times of a 4-cycle with two particles interacting repulsively ($g = +4$) and an altered rate for one of two-way transitions. It is similar to earlier results with the key difference being the transformed time scale. Parameters used: $\beta = 1$, $\varepsilon_i = 0$, number of KMC trajectories: 10^6.

inside the cycle. We observe that the system behaves qualitatively the same as a homogeneous system preserving all symmetries and inequalities outlined in the summary of Sec. 2.1. For single-particle system ($g = 0$), we have discovered a heuristic solution for determining $\tau_0(f, a)$ of a 4-cycle

$$\tau_0(f, a) = \left(\frac{1}{4a} + \frac{3}{4}\right) \tau_0(f, 1). \tag{2.9}$$

For $\tau^{\pm}(f, g, a)$, the above relationship does not hold and can be used only as a rough approximation.

Simulating sites of different energy

Situation is rather fascinating when ε_i are different for individual sites. However, simulating such non-homogeneous systems differs slightly from before. If one were to impose a fixed initial condition $x(t = 0) = x_0$ on a non-homogeneous systems with different ε_i, they would find that $\tau_0^{\pm}(f) \neq \tau_0^{\pm}(-f)$. This is in direct contradiction with theory presented in Sec. 1.3.

To rectify violating equality $\tau_0^{\pm}(f) = \tau_0^{\pm}(-f)$ of system with a single particle, we must determine the initial condition stochastically. That is in accordance with the steady-state probability distribution of NESS.

For a single particle, this corresponds to a probability of occupying certain site. Whereas for multiple-particle system, we must consider all its possible microstates (determined by the position of each particle) and determine the corresponding probabilities.

This is done by letting the system freely evolve from an initial random state to its steady state for an adequately long time (*e.g.* 10^4 individual transitions). We record the time the system spent occupying each possible microstate. Afterwards, we compute steady-state probability by dividing the time spent in a certain microstate by the total time of the simulation. Then for each simulation run, the

system is initialized in some microstate stochastically picked from the computed discrete probability distribution.

High-energy site

In the case when one site has high energy and the interaction is attractive, we observe a sharp increase in $\tau^{\pm}(f)$ and slight increase in $\tau_0(f)$ compared to a homogeneous 4-cycle. The latter is caused only by the difficulty of transitioning over the high-energy site while the former has the added difficulty of the second particle "pulling" onto the first one.

If the interaction is repulsive, we observe $\tau^{\pm}(f)$ decreasing compared to a homogeneous 4-cycle and being similar to those of $\tau_0(f)$. The second particle occupies mostly the low energy sites. Hence, it repels the first particle from occupying them (and vice versa), meaning its presence has the same effect as increasing low sites' overall energy. Yet, as repulsive interaction increases further, we would observe repeated increase in $\tau^{\pm}(f)$ as the second particle starts acting as an extra high-energy site hindering other particles (not plotted).

Inequality (2.3) is preserved for all cases but not as pronounced as in the homogeneous case. Non-homogenities in the process force particles to occupy the lowest energy sites and make it harder for them to move consistently through the whole cycle. It could be argued that an energy landscape of the cycle is more static and the displacement of the second particle tends to 0, in which case the equality of $\tau^{+}(f)$ and $\tau^{-}(f)$ is achieved.

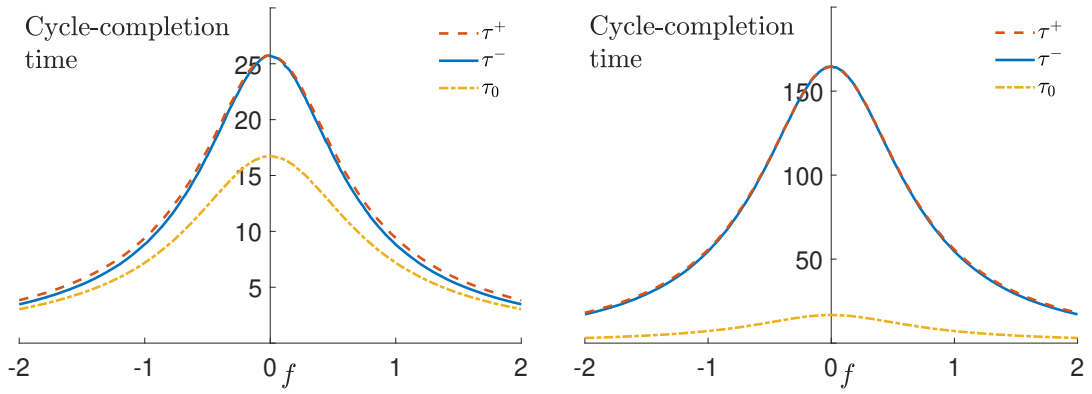

(a) Repulsion $g = +4$ (b) Attraction $g = -4$

Figure 2.8: Cycle-completion times of a 4-cycle with one high-energy site ($\varepsilon = +3$) and two interacting particles. The high-energy site acts as a kinetic barrier slowing down the cycle process; in the case of attractive interaction the most greatly. Parameters used: $\beta = 1$, number of KMC trajectories: 10^6.

Low-energy site

In the case when one site has low energy, a behavior comparable to the high-energy site is demonstrated. For attraction we observe a sharp increase in $\tau^{\pm}(f)$ and slight increase in $\tau_0(f)$ compared to a homogeneous 4-cycle. The second particle

gets trapped in a low-energy site further reducing its energy relative to the other particles. For repulsion, one can instead see the direct analogy of the particle filling a vacancy. As such, $\tau_0(f)$ is significantly bigger than $\tau^{\pm}(f)$ because a particle is not as likely to get trapped in the low-energy site already occupied by the other particle. If $g \gg \varepsilon_i$, then the particle trapped in the low-energy site starts acting instead as a stationary high-energy site.

The cycle-completion time inequality (2.3) is analogous to the high-energy site. Though in this case, second particle's movement is chiefly restricted to only one site instead of three, further weakening the inequality.

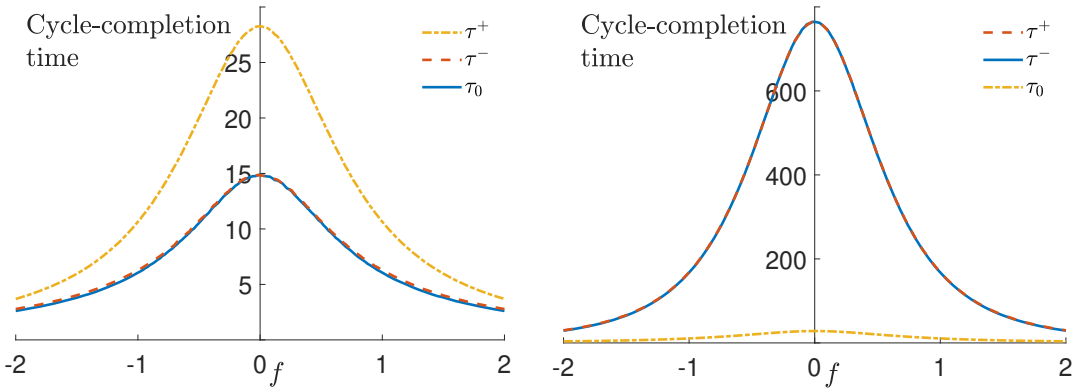

(a) Repulsion $g = +4$ (b) Attraction $g = -4$

Figure 2.9: Cycle-completion times of a 4-cycle with one low-energy site ($\varepsilon = -3$) and two interacting particles. The high-energy site acts as an energy well and most of the time is occuppied by one of the particles. Thus, repulsive interaction expedites the cycle process, while attraction slows it down. Parameters used: $\beta = 1$, number of KMC trajectories: 10^6.

Effect of additional particles

Additional repulsive particles mitigate the effect of different sites' energies as they gradually fill out lowest-energy sites smoothing out the energy landscape and approaching the homogeneous model. Attractive particles on the other hand exacerbate the problem with increasing $\tau^{\pm}(f)$ as they fill out lowest-energy states and make them even lower in relation to other particles.

Inequality (2.3) becomes stronger with an increasing number of particles in the system and the resulting plot of cycle-completion times is qualitatively analogous to Fig. 2.1 and 2.2. It must be noted, however, that in an environment with many particles with a weak interaction, regardless of its nature, events of particles meeting are extremely likely or even inevitable and thus inequality of $\tau^{\pm}(f)$ is instead weakened. When the relative difference of $\tau^+(f)$ and $\tau^-(f)$ is maximal, depends on the number of particles, length of the cycle network and the value of the interaction parameter.

3. Cyclic reactions strongly coupled to reservoirs

In the previous chapter, we have studied n-site unicyclic networks with two or more particles and corresponding cycle-completion times. Can we observe the $\tau^{\pm}(f)$ inequality outside a one-dimensional cyclic reaction network? And equally importantly, are conclusions drawn in the previous chapter still applicable?

To determine behavior of a cyclic reaction in two dimensions, we will use a simple model whose schematic is shown in Fig. 3.1. There are 4×4 states laid out on an orthogonal grid. In the middle, four (blue) lattice sites form a 4-cycle. Single-particle transition rates between the 4-cycle sites are defined in (1.3). The number of particles within the 4-cycle is conserved and equal to one, and the particle is tagged.

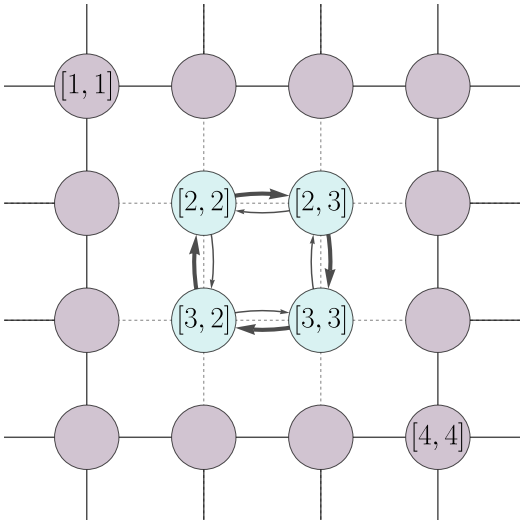

Figure 3.1: Schematic of a cyclic reaction (blue) coupled to an environment (grey). States are labelled according to their position on the dashed grid and emboldened graph edges represent transitions favored by the positive value of drift f.

All other lattice sites (grey circles) represent an ambient environment (a reservoir) which is populated by one or more reservoir particles. Reservoir particles can interact with the tagged particle but not among each other.

A reservoir particle interacts with the tagged particle if the two are located on the nearest or second-nearest neighboring sites. Their interaction energy will again be denoted by g. The rate W_{ij} of the transition, where a particle jumps from the site i to the site j depends on the position of the other particles in the following manner:

$$W_{ij} = \begin{cases} w_{ij} \mathrm{e}^{\frac{\beta}{2} g} & \text{if the site } i \text{ neighbors an occupied reservoir site,} \\ w_{ij} \mathrm{e}^{-\frac{\beta}{2} g} & \text{if the site } j \text{ neighbors an occupied reservoir site,} \\ w_{ij} & \text{if none of the above.} \end{cases} \tag{3.1}$$

We will discriminate between two types of reservoirs. First, the *canonical* reservoir with a constant number of reservoir particles will be considered in Section 3.1. Second, the *grand-canonical* reservoir, where particles can only enter/exit with rates controlled by a prescribed chemical potential will be discussed in Section 3.2.

The main findings are as follows:

i) Inequality (2.2) expressing inhibiting character of interaction on $\tau^{\pm}(f)$ holds in both studied reservoir models.

ii) Inequality (2.3) of cycle-completion times $\tau^{\pm}(f)$ holds in both studied reservoir models.

iii) Inequalities (2.3) and (2.2) are overall less pronounced in the two-dimensional case when compared to the unicyclic model with the same g.

iv) Inequality (2.3) is stronger for attractive interaction compared to a repulsive one (with the same $|g|$).

v) Limits (2.5) and (2.6), for $\tau^{-}(f)$ and $\tau^{+}(f)$, hold in the same manner.

vi) Fluctuations of cycle-completion times are most noticeable in the absence of drift ($f = 0$) and exponentially decrease with increasing $|f|$.

3.1 Canonical reservoir

In the case of a canonical reservoir, we have set the number of reservoir particles to one. In addition, we assume periodic boundary condition, *i.e.*, the particle can move in a single transition from one side of the reservoir to the opposite side.

The particle is free to move between grey lattice sites shown in Fig. 3.1. A rate of any transition in a reservoir is uniform: $w_{ij} = 1$ (comparable to those of the tagged particle). Rates w_{ij} inside reservoir are also subject to the interaction energy between particles and as such, are modified as in Eq. (3.1).

Results of the simulation can be seen in Fig. 3.2 for repulsive and attractive interaction between particles. We indeed do see the inequality of $\tau^{\pm}(f)$ although it is less pronounced than in the one-dimensional lattice. The effect is most appreciable for a reaction strongly coupled to a reservoir.

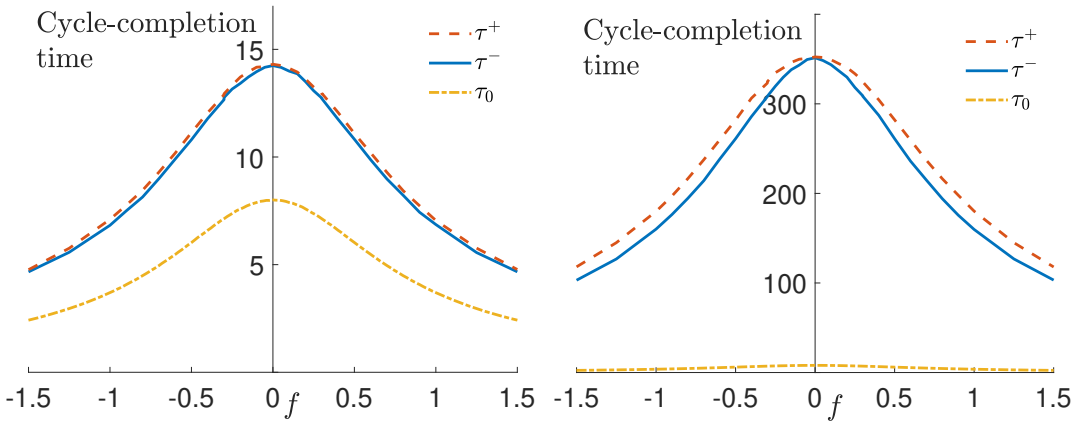

(a) Repulsion $g = +5$ (b) Attraction $g = -5$

Figure 3.2: Cycle-completion times of a 4-cycle populated by one tagged particle embedded in a lattice and interacting with one other particle in a canonical reservoir. Parameters used: $a_{ij} = 1$, $\beta = 1$, number of KMC trajectories: 10^5.

By switching from a very constrained 1D model (only four sites with three of them always in the scope of interaction) to a 2D model, the number of microstates of the system steeply increases. A majority of these microstates is classified as

a situation where no interaction is happening. Thus, the average amount of interaction per trajectory is overall reduced and the inequality (2.3) is weakened.

Interestingly enough, we observe a stronger $\tau^{\pm}(f)$ inequality for an attraction, in contrast to the same value of g for a repulsion. While a repulsive interaction between particles leads to them moving away from each other and being separated, an attractive interaction does the opposite. Attracting particles tend to follow each other moving in tandem; any interaction increases the likelihood of interaction in the future. Analogically to argument asserted in Sec. 2.3, the inequality $\tau^{\pm}(f)$ is caused by the disproportionate number of interaction occurences happening for a cycle completed in the bias direction compared to a cycle completed against the bias. However, if the number of interactions is not high enough at the outset, neither can be the considered disproportion.

To counter the effect of increasing number of no-interaction microstates, either a very strong coupling or an additional reservoir particles are required. Naturally reducing size of the reservoir is also a possible solution to reducing the number of microstates and preserving the inequality (2.3).

3.2 Grand-canonical reservoir

Major portion of cellular machinery functions in a state of constant material exchange with the surrounding environment as particles chemically bind and unbind transferring energy necessary for the cycle to continue. As such, the system can come into contact with an immense number of particles going in and out. Some of these can directly interact with the cycle kinetics. Could $\tau^{\pm}(f)$ inequality manifest even in the case of an open reservoir, in a grand-canonical sense?

In Sec. 3.1 we have proven that $\tau^{\pm}(f)$ inequality does indeed persist if a reservoir particle is free to move inside a reservoir. We shall use the same model as in Fig. 3.1 but with a few modifications aimed at eliminating the possibility of particles moving inside the reservoir.

The particle's movement is reduced exclusively to either entering or exiting some site in the reservoir. These two processes have rates w_{in} and w_{out} associated with them. Rates for either vacating or entering reservoir apply to all states in it. Therefore, there can be multiple particles present in the reservoir, but never more than one in one site. We define w_{in} and w_{out} as follows,

$$\begin{aligned} w_{\text{in}} &= \varrho, \\ w_{\text{out}} &= 1. \end{aligned} \tag{3.2}$$

Parameter ϱ represents a relative occupancy of reservoir sites and corresponds to a chemical potential.

Modification of rates w_{ij} in the case of interaction between the tagged particle and a reservoir particle is handled as stated in Definition (3.1). Explicitly, the reservoir rates W_{ij} of the transition $i \to j$, depend on the position of the tagged

particle in the following manner:

$$W_{\text{in}} = \begin{cases} w_{\text{in}} \mathrm{e}^{\frac{\beta}{2} g} & \text{if a neighboring site is occupied by the tagged particle,} \\ w_{\text{in}} & \text{otherwise.} \end{cases}$$
$$W_{\text{out}} = \begin{cases} w_{\text{out}} \mathrm{e}^{-\frac{\beta}{2} g} & \text{if a neighboring site is occupied by the tagged particle,} \\ w_{\text{out}} & \text{otherwise.} \end{cases} \tag{3.3}$$

Results of computed $\tau^{\pm}(f)$ are shown in Fig. 3.3 for a repulsive and an attractive interaction. The inequality (2.3) is still present although faint. Moreover, we see a trend of a stronger inequality for an attraction in contrast to a repulsion, as similarly observed in the canonical reservoir.

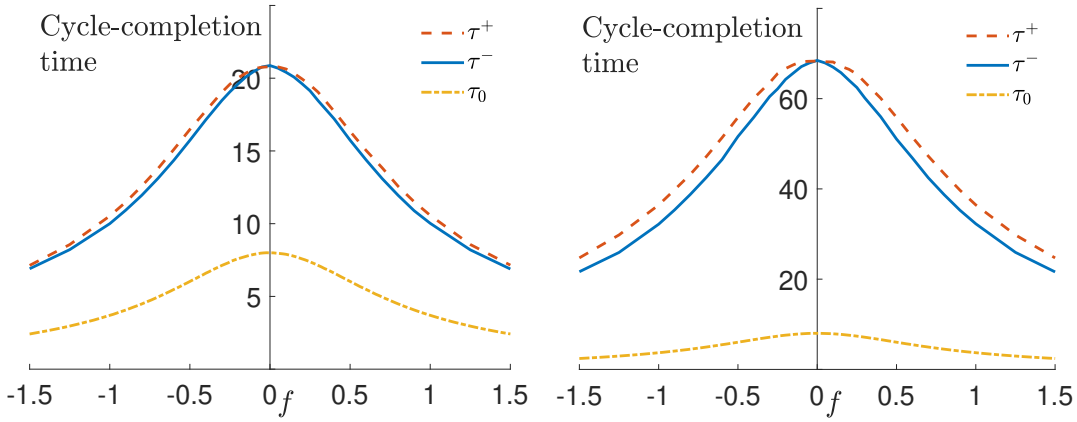

(a) Repulsion $g = +5$ (b) Attraction $g = -5$

Figure 3.3: Cycle-completion times of a 4-cycle populated by one tagged particle embedded in a lattice and interacting with particles in the grand-canonical reservoir. Parameters used: $a_{ij} = 1$, $\beta = 1$, $\varrho = 0.5$, number of KMC trajectories: 1.6×10^5.

Conclusions and Perspectives

Using the kinetic Monte Carlo method, we have studied a unicyclic network with multiple interacting particles. In particular, we have focused on a behavior of mean and variances of cycle-completion times $\tau^{\pm}(f)$ which characterize the cyclic reaction kinetics. In single-particle systems, equality $\tau_0^+(f) = \tau^{0(f)}$ holds for arbitrary transition rates within the cycle. However, systems with two or more particles exhibit a remarkable inequality of cycle-completion times which we verified for several modifications of the model. Counterintuitively, trajectories completing the cycle against the net bias are always (on average) faster than the ones traveling along the bias direction.

Disparity between cycle-completion times occurs due to a smaller amount of interparticle interactions happening in trajectories traveling against the bias. In Chapter 2, we have provided a complete physical picture underlying this phenomenon for both homogeneous and non-homogeneous cycles. Overall, for cycles with sites of vastly different energies, the disparity can be weakened but never entirely eliminated.

In Chapter 3, we have proposed a 2D model of a cyclic reaction and its surroundings to ascertain whether our previous findings can be generalized to systems interacting strongly with an ambient environment. We have considered canonical and grand-canonical reservoirs and come to the same $\tau^{\pm}(f)$ inequality as before. Though it is weaker compared to that of a one-dimensional lattice. We have deduced the reason to be the increased number of microstates with no interparticle interaction. As such, the dynamics of a particle on the cycle approaches that of the single non-interacting particle where $\tau_0^{\pm}(f)$ equality holds.

In future work, it would be interesting to investigate cycle-completion times in models with long-ranged forces or/and non-Markovian dynamics. The former would directly address the universality of observed inequality and shed a new light on its dependence on the interaction force. The latter could lead to new effects caused by a non-negligible memory frequently occurring in the molecular dynamics.

Our results verify a universality of cycle-completion times inequality. In the framework of single isolated processes, such effect might be understably neglible. But in cellular conditions, with up to thousands or even tens of thousands reactions every second occuring simultaneously, its significance could rise considerably. Thus, the most affected reactions should be the most frequent ones, this includes DNA transcription and translation, protein synthesis in ribosomes, processes powered by ATP hydrolysis and others. A necessary condition to observe the predicted phenomenon experimentally, is to have a sufficient statistical sample of unfavorable steps against the bias direction. Therefore, we believe, that our results can be directly observable in reactions with shorter cycles and not very large (compared to $\mathrm{k_B}T$) free energy differences between individual states.

Bibliography

[1] H. Qian and D. A. Beard. Thermodynamics of stoichiometric biochemical networks in living systems far from equilibrium. *Biophys. Chem.*, 114(2):213–220, 2005.

[2] U. Seifert. Stochastic thermodynamics, fluctuation theorems and molecular machines. *Rep. Prog. Phys.*, 75(12):126001, 2012.

[3] M. Bonora, S. Patergnani, A. Rimessi, E. De Marchi, J. M. Suski, A. Bononi, C. Giorgi, S. Marchi, S. Missiroli, F. Poletti, M. R. Wieckowski, and P. Pinton. ATP synthesis and storage. *Purinergic Signal.*, 8(3):343–357, 2012.

[4] G. A. Brooks, T. D. Fahey, and K. Baldwin. *Exercise Physiology: Human Bioenergetics and Its Applications*. McGraw Hill Education, Columbus, 4th edition, 2004.

[5] C. M. Pickart and W. P. Jencks. Energetics of the calcium-transporting ATPase. *J. Biol. Chem.*, 259(3):1629–1643, 1984.

[6] G. A. Brooks. Mammalian fuel utilization during sustained exercise. *Comp. Biochem. Physiol. B*, 120(1):89–107, 1998.

[7] G. A. Gaesser and G. A. Brooks. Muscular efficiency during steady-rate exercise: effects of speed and work rate. *J. Appl. Physiol.*, 38(6):1132–1139, 1975.

[8] J.-R. Yang, X. Chen, and J. Zhang. Codon-by-Codon Modulation of Translational Speed and Accuracy Via mRNA Folding. *PLOS Biology*, 12(7):e1001910, 2014.

[9] T. L. Hill. Studies in irreversible thermodynamics IV. diagrammatic representation of steady state fluxes for unimolecular systems. *J. Theor. Biol.*, 10(3):442–459, 1966.

[10] T. L. Hill. *Free Energy Transduction and Biochemical Cycle Kinetics*. Dover Publications, Minneola, 2004.

[11] J. Schnakenberg. Network theory of microscopic and macroscopic behavior of master equation systems. *Rev. Mod. Phys.*, 48(4):571–585, 1976.

[12] J. E. Molloy and C. Veigel. Myosin Motors Walk the Walk. *Science*, 300(5628):2045–2046, 2003.

[13] R. A. Cross. Myosin's mechanical ratchet. *PNAS*, 103(24):8911–8912, 2006.

[14] D. D. Hackney. The tethered motor domain of a kinesin-microtubule complex catalyzes reversible synthesis of bound ATP. *PNAS*, 102(51):18338–18343, 2005.

[15] H. Itoh, A. Takahashi, K. Adachi, H. Noji, R. Yasuda, M. Yoshida, and K. Kinosita. Mechanically driven ATP synthesis by F 1 -ATPase. *Nature*, 427(6973):465–468, 2004.

[16] B. Derrida. Non-equilibrium steady states: fluctuations and large deviations of the density and of the current. *J. Stat. Mech.*, 2007(07):P07023–P07023, 2007.

[17] R. D. Astumian. Design principles for Brownian molecular machines: how to swim in molasses and walk in a hurricane. *Phys. Chem. Chem. Phys.*, 9(37):5067–5083, 2007.

[18] B. Zhang, D. Jasnow, and D. Zuckerman. Transition-Event Durations in One Dimensional Activated Processes. *J. Chem. Phys.*, 126:074504, 2007.

[19] A. M. Berezhkovskii, M. A. Pustovoit, and S. M. Bezrukov. Channel-facilitated membrane transport: Average lifetimes in the channel. *J. Chem. Phys.*, 119(7):3943–3951, 2003.

[20] H. Qian and X. S. Xie. Generalized Haldane equation and fluctuation theorem in the steady-state cycle kinetics of single enzymes. *Phys. Rev. E*, 74(1):010902, 2006.

[21] A. B. Kolomeisky, E. B. Stukalin, and A. A. Popov. Understanding mechanochemical coupling in kinesins using first-passage-time processes. *Phys. Rev. E*, 71(3):031902, 2005.

[22] M. Lindén and M. Wallin. Dwell Time Symmetry in Random Walks and Molecular Motors. *Biophys. J.*, 92(11):3804–3816, 2007.

[23] W. Hwang and C. Hyeon. Energetic Costs, Precision, and Transport Efficiency of Molecular Motors. *J. Phys. Chem. Lett.*, 9(3):513–520, 2018.

[24] A. Dutta, G. M. Schütz, and D. Chowdhury. Stochastic thermodynamics and modes of operation of a ribosome: A network theoretic perspective. *Phys. Rev. E*, 101(3):032402, 2020.

[25] V. Wolf. Modelling of Biochemical Reactions by Stochastic Automata Networks. *Electron. Notes Theor. Comput. Sci.*, 171(2):197–208, 2007.

[26] N. G. V. Kampen. *Stochastic Processes in Physics and Chemistry*. Elsevier, Amsterdam, 2011.

[27] D. Colquhoun, K. A. Dowsland, M. Beato, and A. J. R. Plested. How to Impose Microscopic Reversibility in Complex Reaction Mechanisms. *Biophys. J.*, 86(6):3510–3518, 2004.

[28] A. O'Hagan and J. J. Forster. *Kendall's Advanced Theory of Statistics, volume 2B: Bayesian Inference*, volume 2B. Hodder Arnold, London, 2nd edition, 2004.

[29] C. Maes and K. Netočný. Time-Reversal and Entropy. *J. Stat. Phys.*, 110(1):269–310, 2003.

[30] W. Min, L. Jiang, J. Yu, S. C. Kou, H. Qian, and X. S. Xie. Nonequilibrium Steady State of a Nanometric Biochemical System: Determining the Thermodynamic Driving Force from Single Enzyme Turnover Time Traces. *Nano Lett.*, 5(12):2373–2378, 2005.

[31] W. Feller. *An Introduction to Probability Theory and Its Applications*, volume 1. Wiley, New York, 3rd edition, 1968.

[32] C. M. Grinstead and J. L. Snell. *Introduction to Probability*. American Mathematical Society, Providence, 2nd edition, 1997.

[33] S. Redner. *A Guide to First-Passage Processes*. Cambridge University Press, Cambridge, 1st edition, 2001.

[34] P. A. Pury and M. O. Cáceres. Mean first-passage and residence times of random walks on asymmetric disordered chains. *J. Phys. A: Math. Gen.*, 36(11):2695–2706, 2003.

[35] B. Meng and W. H. Weinberg. Monte Carlo simulations of temperature programmed desorption spectra. *J. Chem. Phys.*, 100(7):5280–5289, 1994.

[36] D. T. Gillespie. A general method for numerically simulating the stochastic time evolution of coupled chemical reactions. *J. Comput. Phys.*, 22(4):403–434, 1976.

[37] D. T. Gillespie. Exact stochastic simulation of coupled chemical reactions. *J. Phys. Chem.*, 81(25):2340–2361, 1977.

[38] A. Yildiz, J. N. Forkey, S. A. McKinney, T. Ha, Y. E. Goldman, and P. R. Selvin. Myosin V Walks Hand-Over-Hand: Single Fluorophore Imaging with 1.5-nm Localization. *Science*, 300(5628):2061–2065, 2003.

[39] A. M. Berezhkovskii, L. Dagdug, and S. M. Bezrukov. Mean Direct-Transit and Looping Times as Functions of the Potential Shape. *J. Phys. Chem. B*, 121(21):5455–5460, 2017.

[40] A. M. Berezhkovskii, G. Hummer, and S. M. Bezrukov. Identity of Distributions of Direct Uphill and Downhill Translocation Times for Particles Traversing Membrane Channels. *Phys. Rev. Lett.*, 97(2):020601, 2006.

[41] J. Gladrow, M. Ribezzi-Crivellari, F. Ritort, and U. F. Keyser. Experimental evidence of symmetry breaking of transition-path times. *Nat. Commun.*, 10(1):1–9, 2019.

[42] A. Ryabov, D. Lips, and P. Maass. Counterintuitive Short Uphill Transitions in Single-File Diffusion. *J. Phys. Chem.*, 123(9):5714–5720, 2019.

A. Appendix

A.1 Matlab R2019b codes

Code 1: Mean cycle time of a 4-cycle given drift f, interaction parameter g and absorbing boundary.

```
function tau = 4Cycle(f,AbsorbingBoundary,g,mc)
CycleTimeData = zeros(1,mc);
beta = 1;
w = zeros(4);
len = length(w);
%%_________________________RATES FOR PARTICLES_________________________%%
for i = 1:len
    w(i,mod(i,len)+1) = exp(-beta/2*f);
    w(mod(i,len)+1,i) = exp(beta/2*f);
end
%%_____________________________TOTAL RATES_____________________________%%
Z = 2*w(2,1)+ 2*w(1,2);
Zg1 = w(2,1)+ w(1,2)+(w(2,1)+w(1,2))*exp(-beta/2*g);
Zg0 = exp(beta/2*g)*Z;
%%_____________________________INITIAL STATE_____________________________%%
y = randi(4);
x = 1;
%%____________________PICKING ABSORBING BOUNDARY_____________________%%
if AbsorbingBoundary == 1
    OtherAbsorbingBoundary = +len;
    AbsorbingBoundary = -len;
else
    AbsorbingBoundary = len;
    OtherAbsorbingBoundary = -len;
end
%%_________________________MONTE CARLO SIMULATION_________________________%%
for d = 1 : mc
    counter = 0;
    while (counter~=AbsorbingBoundary)
        t = 0;
        counter = 0;
        while (counter~=AbsorbingBoundary && counter~=OtherAbsorbingBoundary)
            ra_1 = rand;
            x_ps = mod(x,len)+1;
            x_ms = mod(x-2,len)+1;
            y_ps = mod(y,len)+1;
            y_ms = mod(y-2,len)+1;
            %%_____________________SAME STATE_____________________%%
            if x == y
                t = t -1/Zg0*log(rand);
                if ra_1 <= w(x_ms,x)/Z
                    counter = counter - 1;
                    x = x_ms;
                elseif ra_1 <= (w(x_ms,x)+w(x_ps,x))/Z
                    counter = counter + 1;
                    x = x_ps;
                elseif ra_1 <= (w(x_ms,x)+w(x_ps,x)+w(y_ms,y))/Z
                    y = y_ms;
                else
                    y = y_ps;
                end
            %%_____________NEIGHBOR STATE (RIGHT)_____________%%
            elseif mod(x-y,len) == 1
                t = t -1/Zg1*log(rand);
                if ra_1 <= w(x_ms,x)*exp(-beta/2*g)/Zg1
                    counter = counter - 1;
                    x = x_ms;
                elseif ra_1 <= (w(x_ms,x)*exp(-beta/2*g)+w(x_ps,x))/Zg1
                    counter = counter + 1;
                    x = x_ps;
                elseif ra_1 <= ((w(x_ms,x)+w(y_ps,y))*exp(-beta/2*g)+w(x_ps,x))/Zg1
                    y = y_ps;
```

```
                else
                    y = y_ms;
                end
            %%__________________NEIGHBOR STATE (LEFT)___________________%%
            elseif mod(x-y,len) == len-1
                t = t -1/Zg1*log(rand);
                if ra_1 <= w(x_ms,x)/Zg1
                    counter = counter - 1;
                    x = x_ms;
                elseif ra_1 <= (w(x_ms,x)+w(x_ps,x)*exp(-beta/2*g))/Zg1
                    counter = counter + 1;
                    x = x_ps;
                elseif ra_1 <= (w(x_ms,x)+(w(x_ps,x)+w(y_ms,y))*exp(-beta/2*g))/Zg1
                    y = y_ms;
                else
                    y = y_ps;
                end
            %%_____________________NO INTERACTION_________________________%%
            else
                t = t -1/Z*log(rand);
                if ra_1 <= w(x_ms,x)/Z
                    x = x_ms;
                    counter = counter - 1;
                elseif ra_1 <= (w(x_ms,x)+w(x_ps,x))/Z
                    x = x_ps;
                    counter = counter + 1;
                elseif ra_1 <= (w(x_ms,x)+w(x_ps,x)+w(y_ps,y))/Z
                    y = y_ps;
                else
                    y = y_ms;
                end
            end
        end
    end
    CycleTimeData(d) = t;
end
tau = mean(CycleTimeData);
end
```

Code 2: Determination of steady-state probabilities of all microstates when cycle is non-homogeneous.

```
...
eps = zeros(1,4);
eps(1) = 0;
eps(2) = 0;
eps(3) = 0;
eps(4) = 0;

for i=1:len
    for j=1:len
        w(j,i) = w(j,i)*exp(beta/2*(eps(i)-eps(j)));
    end
end
a = 1;
w(1,2)=a*w(1,2);
w(2,1)=a*w(2,1);
...
y = randi(len);
x = randi(len);
t = 0;
steady_state_probabilities = zeros(len,len);
%%_________________________INITIAL SIMULATION_________________________%%
for Number_of_Transitions = 1:10000
    t_aux = - 1/Z(x,y)*log(rand);
    t = t + t_aux;
    steady_state_probabilities(x,y) = tprob(x,y) + t_aux;
    ...
    %% Determination of the next microstate %%
    ...
end
```

```
%%_________________DETERMINING MICROSTATE PROBABILITIES_____________%%
steady_state_probabilities = steady_state_probabilities/t;
cumm_probability = zeros(len,len);
for i = 1:len^2
    for j = 1:i
        cumm_probability(i) = cumm_probability(i) + cumm_probability(j);
    end
end
...
%%_________________________MONTE CARLO SIMULATION_________________________%%
for d = 1 : mc
    counter = 0;
    while (counter~=AbsorbingBoundary)
        t = 0;
        counter = 0;
        idx = find(cumm_probality>rand,1);
        [x,y] = ind2sub([len,len],idx);
        while (counter~=AbsorbingBoundary && counter~=OtherAbsorbingBoundary)
...
```

Code 3: Mean cycle-completion time in a 2D lattice model (canonical reservoir).

```
function tau = Tau2D(f1,particles,shape1,shape2,f2,AbsorbingBoundary,g,mc)
CycleTimeData = zeros(1,mc);
beta = 1;
rowsize=shape1(1);
colsize=shape1(2);

%%_________________ALLOWED OCCUPATIONS OF THE SYSTEM_________________%%
mx_RESERVOIR = ones(shape2(1),shape2(2));
mx_RESERVOIR(2:2+rowsize-1,2:2+colsize-1)=zeros(rowsize,colsize);

mx_CYCLE = zeros(shape2(1),shape2(2));
mx_CYCLE(2:2+rowsize-1,2)=ones(rowsize,1);
mx_CYCLE(2:2+rowsize-1,2+colsize-1)=ones(rowsize,1);
mx_CYCLE(2,2:2+colsize-1)=ones(1,colsize);
mx_CYCLE(2+rowsize-1,2:2+colsize-1)=ones(1,colsize,1);

%%_________________TRANSITION RATES FOR CYCLE PARTICLE_________________%%
w_CYCLE = zeros(shape2(1),shape2(2),shape2(1),shape2(2));
i=0;
j=0;
while j<colsize-1
    w_CYCLE(2,2+j+1,2,2+j)= exp(beta/2*f1);
    w_CYCLE(2,2+j,2,2+j+1)= exp(-beta/2*f1);
    j=j+1;
end
while i<rowsize-1
    w_CYCLE(2+i+1,2+j,2+i,2+j)= exp(beta/2*f1);
    w_CYCLE(2+i,2+j,2+i+1,2+j)= exp(-beta/2*f1);
    i=i+1;
end
while j>0
    w_CYCLE(2+i,2+j-1,2+i,2+j)= exp(beta/2*f1);
    w_CYCLE(2+i,2+j,2+i,2+j-1)= exp(-beta/2*f1);
    j=j-1;
end
while i>0
    w_CYCLE(2+i-1,2+j,2+i,2+j)= exp(beta/2*f1);
    w_CYCLE(2+i,2+j,2+i-1,2+j)= exp(-beta/2*f1);
    i=i-1;
end
%%_____________TRANSITION RATES FOR RESERVOIR PARTICLE_____________%%
w_RESERVOIR = zeros(shape2(1),shape2(2),shape2(1),shape2(2));
w_vertic = 1;
for k = 1:shape2(1)
    for l = 1:shape2(2)
        if mx_RESERVOIR(k,l)==0
            continue
        end
        for i = 1:shape2(1)
```

```
            for j = 1:shape2(2)
                if mx_RESERVOIR(i,j)==0
                    continue
                end
                if norm([i,j]-[k,l])==1
                    if j==l
                        w_RESERVOIR(i,j,k,l) = w_vertic;
                    elseif i==k && j-l > 0
                        w_RESERVOIR(i,j,k,l) = exp(beta/2*f2);
                    elseif i==k && j-l < 0
                        w_RESERVOIR(i,j,k,l) = exp(-beta/2*f2);
                    end
                end
                if norm([i,j]-[k,l])==shape2(2)-1
                    if i==k && j-l < 0
                        w_RESERVOIR(i,j,k,l) = exp(beta/2*f2);
                    elseif i==k && j-l > 0
                        w_RESERVOIR(i,j,k,l) = exp(-beta/2*f2);
                    end
                end
                if norm([i,j]-[k,l])==shape2(1)-1
                    if j==l
                        w_RESERVOIR(i,j,k,l) = w_vertic;
                    end
                end
            end
        end
    end
end
%%_____________________LEDGER OF CONFIGURATIONS_____________________%%
numofconfigs = nnz(mx_CYCLE)* nnz(mx_RESERVOIR)^particles;
% linear indices of allowed states - cycle and reservoir
idx1=find(mx_CYCLE);
idx2=find(mx_RESERVOIR);
% combinations: matrix of all poss. combinations (generation of all
% microstates expressed with linear indices)
combinations = {idx1};
for i=1:particles
    combinations{end+1} = idx2;
end
lel = length(combinations);
[combinations{:}] = ndgrid(combinations{end:-1:1});
combinations = cat(lel+1,combinations{:});
combinations = fliplr(reshape(combinations,[],lel));
% ledger (as of yet incomplete) of microstates and their transitions
% 1st column: current microstate,
% 2nd: possible microstates from current microstate,
% 3rd: rates (and later probabiliies)
ledger = zeros(0,3);
for n = 1:numofconfigs
    % cycle particle's position
    [x,y]=ind2sub(size(mx_CYCLE),combinations(n,1));
    % reservoir particle's position
    [xrsv,yrsv]=ind2sub(size(mx_CYCLE),combinations(n,2:(particles+1)));

    idxw1=find(w_CYCLE(:,:,x,y));
    for p=1:length(idxw1)
        [i,j]=ind2sub(size(mx_CYCLE),idxw1(p));
        % vector made up of linear indices describing particles'
        % positions of a certain microstate
        kod = combinations(n,:);
        kod(1)= idxw1(p);
        [~,cislo]=ismember(kod,combinations,'rows');
        ledger = [ledger;n,cislo,w_CYCLE(i,j,x,y)];
        % Application of interaction on rates
        for ch = 1:length(yrsv)
            if norm([i,j]-[xrsv(ch),yrsv(ch)]) == 1
                ledger(end,3)= ledger(end,3)*exp(-beta/2*g);
            end
            if norm([x,y]-[xrsv(ch),yrsv(ch)]) == 1 && norm([i,j]-[xrsv(ch),yrsv(ch)])~=1
                ledger(end,3)= ledger(end,3)*exp(beta/2*g);
            end
        end
```

```
    end

    for m = 2:(particles+1)
        idxw2=find(w_RESERVOIR(:,:,xrsv(m-1),yrsv(m-1)));
        for p=1:length(idxw2)
            [i,j]=ind2sub(size(mx_CYCLE),idxw2(p));
            kod = combinations(n,:);
            kod(m)= idxw2(p);
            [~,cislo]=ismember(kod,combinations,'rows');
            ledger = [ledger;n,cislo,w_RESERVOIR(i,j,xrsv(m-1),yrsv(m-1))];
            if norm([i,j]-[x,y]) == 1
                ledger(end,3)= ledger(end,3)*exp(-beta/2*g);
            end
            if norm([xrsv(m-1),yrsv(m-1)]-[x,y]) == 1 && norm([i,j]-[x,y])~=1
                ledger(end,3)= ledger(end,3)*exp(beta/2*g);
            end
        end
    end
end
% Total rates computation
Z=zeros(1,numofconfigs);
for i=1:numofconfigs
    sum_indexes = find(ledger(:,1)==i);
    for j=sum_indexes'
        Z(i)=Z(i)+ledger(j,3);
    end
    for j=sum_indexes'
        ledger(j,3)= ledger(j,3)/Z(i);
    end
end
%%_____________________PICKING ABSORBING BOUNDARY_____________________%%
if AbsorbingBoundary == 1
    OtherAbsorbingBoundary = 2;
    AbsorbingBoundary = -2;
else
    AbsorbingBoundary = 2;
    OtherAbsorbingBoundary = -2;
end
%%_____________________________INITIAL STATE_____________________________%%
% occupational matrix of states in lattice.
ocp_mx = zeros(shape2(1),shape2(2));
ocp_mx(2,2) = -1;
% setting random initial state
for i=1:particles
    ra_init = randsample(find(mx_RESERVOIR),1);
    ocp_mx(ra_init) = ocp_mx(ra_init)+1;
end
% conversion of matrix with occupational numbers into one single
% microstate index.
init_cycleparticle=find(ocp_mx == -1);
init = find(ocp_mx > 0);
v = nonzeros(ocp_mx);
v = v(v ~= -1);
init_reservoir = zeros(0);
for i = 1:length(init)
    init_reservoir = [init_reservoir,init(i)*ones(1,v(i))];
end
init = [init_cycleparticle,init_reservoir];
[~,init_number]=ismember(init,combinations,'rows');
current_number = init_number;
%%_____________________________MONTE CARLO_____________________________%%
for d = 1 : mc
    counter = 0;
    t = 0;
    while (counter ~= AbsorbingBoundary)
        t = 0;
        counter = 0;
        while (counter ~= AbsorbingBoundary && counter ~= OtherAbsorbingBoundary)
            t = t -1/Z(current_number)*log(rand);
            previous_number = current_number;
            %%%__________NEW CONFIGURATION_________%%%
            ra_1 = rand;
            indxnpconfigs = find(ledger(:,1)==current_number);
```

```
            npconfigs = ledger(indxnpconfigs,2);
            cumm_probability = 0;
            for i = 1:length(indxnpconfigs)
                cumm_probability = cumm_probability + ledger(indxnpconfigs(i),3);
                if ra_1 <= cumm_probability
                    current_number=npconfigs(i);
                    %%____________________COUNTER_____________________%%
                    if i == 1 || i == 2
                        cycleold = combinations(previous_number,1);
                        cyclenew = combinations(current_number,1);
                        [oldrow,oldcol]=ind2sub(size(mx_CYCLE),cycleold);
                        [newrow,newcol]=ind2sub(size(mx_CYCLE),cyclenew);
                        if [oldrow,oldcol] == [2,2]
                            if [newrow,newcol] == [2,3]
                                counter = counter + 1;
                            elseif [newrow,newcol] == [3,2]
                                counter = counter - 1;
                            end
                        end
                        if [newrow,newcol] == [2,2]
                            if [oldrow,oldcol] == [2,3]
                                counter = counter - 1;
                            elseif  [oldrow,oldcol] == [3,2]
                                counter = counter + 1;
                            end
                        end
                    end
                    break
                end
            end
        end
    end
    CycleTimeData(d) = t;
end
tau = mean(CycleTimeData);
end
```

Code 4: Mean cycle-completion time in a 2D lattice model with particles only entering and exiting reservoir (grand-canonical reservoir).

```
function u = TauGrand(f,AbsorbingBoundary,rho,g,mc)
CycleTimeData = zeros(1,mc);
beta = 1;
w = zeros(4);
len = length(w);
rsv = [1,2;
       1,3;
       2,4;
       3,4;
       4,3;
       4,2;
       3,1;
       2,1];
w_OUT = ones(1,8);
w_IN = rho*ones(1,8);
%%_____________________________INITIAL STATE_____________________________%%
near_states = rho*exp(-beta*g);
sumgrand = 2*near_states+6*rho;
rho = rho/sumgrand;
near_states = near_states/sumgrand;
occupied_rsv_indexes = [];
for i = 1:8
    if norm(rsv(i,:)-[2,2]) == 1
        if rand <= near_states
            occupied_rsv_indexes = [occupied_rsv_indexes,i];
        end
    else
        if rand <= rho
            occupied_rsv_indexes = [occupied_rsv_indexes,i];
        end
    end
```

```
end
x = 1;
%%_________________________CYCLE TRANSITION RATES_________________________%%
for i = 1:len
    w(i,mod(i,len)+1) = exp(-beta/2*f);
    w(mod(i,len)+1,i) = exp(beta/2*f);
end
%%_____________________PICKING ABSORBING BOUNDARY_____________________%%
if AbsorbingBoundary == 1
    OtherAbsorbingBoundary = (len)*(1);
    AbsorbingBoundary = (len)*(-1);
else
    AbsorbingBoundary = (len)*(1);
    OtherAbsorbingBoundary = (len)*(-1);
end
%%_________________________MONTE CARLO SIMULATION_________________________%%
for d = 1 : mc
    counter = 0;
    t = 0;
    while (counter~=AbsorbingBoundary)
            t = 0;
            counter = 0;
        while (counter~=AbsorbingBoundary && counter~=OtherAbsorbingBoundary)
            x_ps = mod(x,len)+1;
            x_ms = mod(x-2,len)+1;
            w_ps = w(x_ps,x);
            w_ms = w(x_ms,x);
            [x1,x2] = cycind(x);
            x_ind = [x1,x2];
            [x1,x2] = cycind(x_ps);
            x_ind_ps = [x1,x2];
            [x1,x2] = cycind(x_ms);
            x_ind_ms = [x1,x2];
            % Interaction modification of cycle particle rates
            for i = occupied_rsv_indexes
                if norm(rsv(i,:)-x_ind) == 1
                    w_ps = w_ps*exp(beta/2*g);
                    w_ms = w_ms*exp(beta/2*g);
                elseif norm(rsv(i,:)-x_ind_ps) == 1
                    w_ps = w_ps*exp(-beta/2*g);
                elseif norm(rsv(i,:)-x_ind_ms) == 1
                    w_ms = w_ms*exp(-beta/2*g);
                end
            end
            % Interaction modification of reservoir rates
            w_rsv = ones(1,8);
            for i = 1:8
                if ~ismember(i,occupied_rsv_indexes)
                    if norm(rsv(i,:)-x_ind) == 1
                        w_rsv(i)=w_IN(i)*exp(-beta/2*g);
                    else
                        w_rsv(i) = w_IN(i);
                    end
                else
                    if norm(rsv(i,:)-x_ind) == 1
                        w_rsv(i) = w_OUT(i)*exp(beta/2*g);
                    else
                        w_rsv(i) = w_OUT(i);
                    end
                end
            end
            Z = w_ps + w_ms + sum(w_rsv);
            t = t - 1/Z*log(rand);
            ra1 = rand;
            % Transitions in the cycle
            if ra1 <= w_ps/Z
                counter = counter + 1;
                x = x_ps;
                continue
            elseif ra1 <= (w_ps+w_ms)/Z
                counter = counter - 1;
                x = x_ms;
                continue
```

```
            end
            % Transitions in the reservoir
            cumm_Z = w_ps + w_ms;
            for i = 1:8
                if ra1 <= (cumm_Z + w_rsv(i))/Z
                    if ismember(i,occupied_rsv_indexes)
                        occupied_rsv_indexes = occupied_rsv_indexes(occupied_rsv_indexes~=i);
                    else
                        occupied_rsv_indexes = [occupied_rsv_indexes,i];
                    end
                    break
                else
                    cumm_Z = cumm_Z + w_rsv(i);
                end
            end
        end
    end
CycleTimeData(d) = t;
end
u = mean(CycleTimeData);
end
```

Code 5: Auxilliary function transforming linear indices to subscripts.

```
function [x1,x2] = cycind(l)
switch l
    case 1
        x1 = 2;
        x2 = 2;
    case 2
        x1 = 2;
        x2 = 3;
    case 3
        x1 = 3;
        x2 = 3;
    case 4
        x1 = 3;
        x2 = 2;
    otherwise
         warning('index is out of 1-4 bounds!')
end
end
```